

Supplementary information:

Tuning the electronic environment of cations and anions using ionic liquid mixtures

Ignacio J. Villar-Garcia, Kevin R. J. Lovelock, Shuang Men and Peter Licence**

*The School of Chemistry
The University of Nottingham
Nottingham
NG7 2RD, UK.*

*To whom correspondence should be addressed:


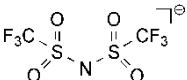
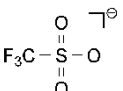
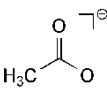
i.villar-garcia@imperial.ac.uk; +44 (0) 7827767149
pete.licence@nottingham.ac.uk; +44 (0) 115 846 6176. Fax: +44 (0)115 9513563

Experimental

Materials: The ionic liquids investigated in this study were all prepared in our laboratory *via* established synthetic methods: $[\text{C}_8\text{C}_1\text{Im}]\text{Cl}$,¹ $[\text{C}_8\text{C}_1\text{Im}][\text{Tf}_2\text{N}]$,² $[\text{C}_8\text{C}_1\text{Im}][\text{TfO}]$,³ $[\text{C}_8\text{C}_1\text{Im}][\text{OAc}]$.⁴ Unless otherwise stated, all ionic liquids were characterised by ESI-MS (Bruker MicroTOF) and both ^1H and ^{13}C NMR spectra were recorded on a Bruker DPX-400 spectrometer at 400 and 101 MHz respectively as solutions in either CDCl_3 or $\text{MeOD-}d_4$. When anion exchange was one of the synthetic steps, ion chromatography analysis showed that halide concentration was < 10 ppm for $[\text{C}_8\text{C}_1\text{Im}][\text{Tf}_2\text{N}]$ and < 1000 ppm for $[\text{C}_8\text{C}_1\text{Im}][\text{TfO}]$ and $[\text{C}_8\text{C}_1\text{Im}][\text{OAc}]$ respectively. Furthermore, the absence of additional photoemission envelopes corresponding to residual halide, Li^+ and Si (known to originate from surface segregated silicones) confirmed the purity of the substrate, ensuring suitability for further study, *i.e.*, the concentration in each case was below the limit of detection of the instrumentation.

Preparation of ionic liquid mixtures: The ionic liquid mixtures investigated in this study were prepared in our laboratory by mixing the appropriate gravimetric quantities of high-purity substituent neat ionic liquids. Each ionic liquid-based mixture was stirred for 60 min under vacuum ($p \approx 10^{-2}$ mbar) to avoid ingress of atmospheric gases and water. Furthermore, each sample was inspected to ensure that it was a single homogeneous liquid phase before further investigation by XPS.

Table S1. Structure and abbreviations of the polynuclear ions investigated in this study, **note:** chloride (Cl-) based samples are also studied.

Abbreviation	Structure	Name
$[\text{C}_8\text{C}_1\text{Im}]^+$		1-octyl-3-methylimidazolium
$[\text{Tf}_2\text{N}]^-$		Bis[(trifluoromethyl)sulfonyl]imide
$[\text{TfO}]^-$		Trifluoromethanesulfonate
$[\text{OAc}]^-$		Acetate

Preparation of Pd Containing Ionic Liquid Solutions: All ionic liquid solutions were prepared in an inert atmosphere (Ar) using pre-pumped and de-gassed ionic liquids. Into a mixture of NaCl (12mg, 0.21mmol), bromobenzene (13.1ml, 0.125 mmol) and [Pd(PPh₃)₄] (24 mg, 0.021 mmol) in [C₈C₁Im][OAc] (0.25 ml), a solution of Na₂CO₃ (26 mg, 0.25 mmol) in water (0.125 ml) was injected. The resulting solution was heated to 110 °C for 3 h to ensure complete dissolution of the organometallic species. All undissolved materials were removed by filtration and all volatiles removed *in vacuo*.

Suzuki cross-coupling reactions: A mixture of NaCl (38 mg, 0.67 mmol), phenylboronic acid (0.58 g, 4.76 mmol) and [Pd(PPh₃)₄] (5.5 mg, 4.76 × 10⁻³ mmol) in 2 mL of ionic liquid was stirred at 110 °C. Into this mixture, a solution of Na₂CO₃ (83 mg, 0.783 mmol) in water (3 mL) and bromobenzene (0.5 mL, 4.76 mmol) were injected. The reaction was allowed to proceed at 110 °C for 10 minutes. Immediately after this time, the mixture was cooled using liquid nitrogen to stop reaction. **Reaction conversion** in all cases was monitored by ¹H NMR. The proton signals from both of the starting materials and the product show similar chemical shift (δ), between 7.65 and 7.15 ppm. However, the two ortho-protons within phenylboronic acid show higher δ at around 8.00 ppm and therefore can be easily integrated to quantify the conversion. The reaction conversion calculated by integrating the desired ¹H NMR peaks was consequently used to calculate the *Turnover of Frequency* (TOF) of the reaction. It is given in the following equation:

$$TOF = \frac{\text{mol of starting material converted}}{\text{mol of catalyst} \times \text{time}} = \frac{\text{conversion}}{0.1 \% \times \text{time}}$$

It must be noted that the TOF was given by assuming that no side reaction was carried out during the reaction, and thus the starting materials will only be converted to the desired product. NMR spectroscopy suggests that this assumption is valid as all observed peaks can be assigned to the starting materials, product or the solvent.

XPS Data Collection: All XP spectra were recorded using a Kratos Axis Ultra spectrometer employing a focused, monochromated Al K α source ($h\nu = 1486.6$ eV), hybrid (magnetic/electrostatic) optics, hemispherical analyser and a multi-channel plate

and delay line detector (DLD) with an X-ray incident angle of 30° (relative to the surface normal). X-ray gun power was set to 100 W. All spectra were recorded using an entrance aperture of $300 \times 700 \mu\text{m}$ with a pass energy of 80 eV for survey spectra and 20 eV for high-resolution spectra. The instrument sensitivity was 7.5×10^5 counts s^{-1} when measuring the Ag $3d_{5/2}$ photoemission peak for an atomically clean Ag sample recorded at a pass energy of 20 eV and 450 W emission power. Ag $3d_{5/2}$ full width at half maximum (FWHM) was 0.55 eV for the same instrument settings. Binding energy calibration was made using Au $4f_{7/2}$ (83.96 eV), Ag $3d_{5/2}$ (368.21 eV) and Cu $2p_{3/2}$ (932.62 eV). The absolute error in the acquisition of binding energies is ± 0.1 eV, as quoted by the instruments manufacturer (Kratos); consequently, any binding energies within 0.2 eV can be considered the same, within the experimental error. Charge neutralisation methods were not required (or employed) in the measurement of these data. Sample stubs were earthed through the instrument stage using a standard BNC connector. Samples were prepared by placing a small drop (≈ 20 mg) of the ionic liquid into a depression on a stainless steel sample stub (designed for powders) or on a standard stainless steel multi-sample bar (both Kratos designs). The ionic liquid samples were then cast into thin films *ex situ* (approx. thickness 0.5 – 1 mm). Initial pumping to high vacuum was carried out in a preparation chamber immediately after thin film preparation to avoid significant absorption of atmospheric gases and other volatile impurities. The preparation chamber pressure was $\approx 10^{-7}$ mbar. Pumping-times varied (1 – 3 hr total) depending upon the volume, volatile impurity content and viscosity of the sample, *i.e.*, viscous ionic liquids were found to require longer pumping times. The samples were then transferred to the main analytical vacuum chamber, the pressure of which remained $\leq 1 \times 10^{-8}$ mbar during the measurement of all XP spectra. The low chamber pressure suggests that all volatile impurities, such as water, are highly likely to be removed, leading to high purity samples.⁵

XPS Data Analysis: For data interpretation, a two point linear subtraction was used; for $[\text{Tf}_2\text{N}]^-$ based ionic liquids the C 1s XP spectra were subtracted using a linear spline to allow for the CF_3 substituent. Relative Sensitivity Factors (RSF) were taken from the Kratos Library (where RSF of F 1s = 1.000) and were used to calculate observed atomic percentages.⁶ Peaks were fitted using GL(30) lineshapes; a combination of a Gaussian (70%) and Lorentzian (30%).^{6a,7} This lineshape has been used consistently in the fitting

of XP spectra, and has been found to match experimental lineshapes in ionic liquid systems.^{6a,8} All XP spectra were charge corrected by referencing the aliphatic C 1s photoemission peak (C_{alkyl} 1s) to 285.0 eV, this simple procedure was valid as the alkyl substituent was long, i.e. $n \geq 8$.^{8a}

Characterisation of an example of a mixture of ionic liquids: Figure S1 shows an example of a survey scan XP spectrum, in this case for the equimolar mixture (1:1) of [C₈C₁Im]Cl and [C₈C₁Im][Tf₂N] ([C₈C₁Im]Cl_{0.5}[Tf₂N]_{0.5}). Photoemission envelopes are observed for each of the expected elements, as is indeed the case for all of the ionic liquid-based samples presented herein. Previous studies of imidazolium-based ionic liquids by XPS have highlighted the presence of silicone-based impurities and oxygenates in the near-surface region that could not be detected using NMR spectroscopy or other bulk sensitive techniques.^{6a,9} Consequently, the survey spectra were examined thoroughly to ensure that surface segregated impurities of this type, which may act as surfactants, were not present as these could possibly lead to ordering or speciation in mixture based systems.

The survey scans also confirmed that the samples were free of both residual halide and lithium contamination which could be carried over from ion exchange chemistries employed in synthesis (Figure S1 and Figures S3-6).

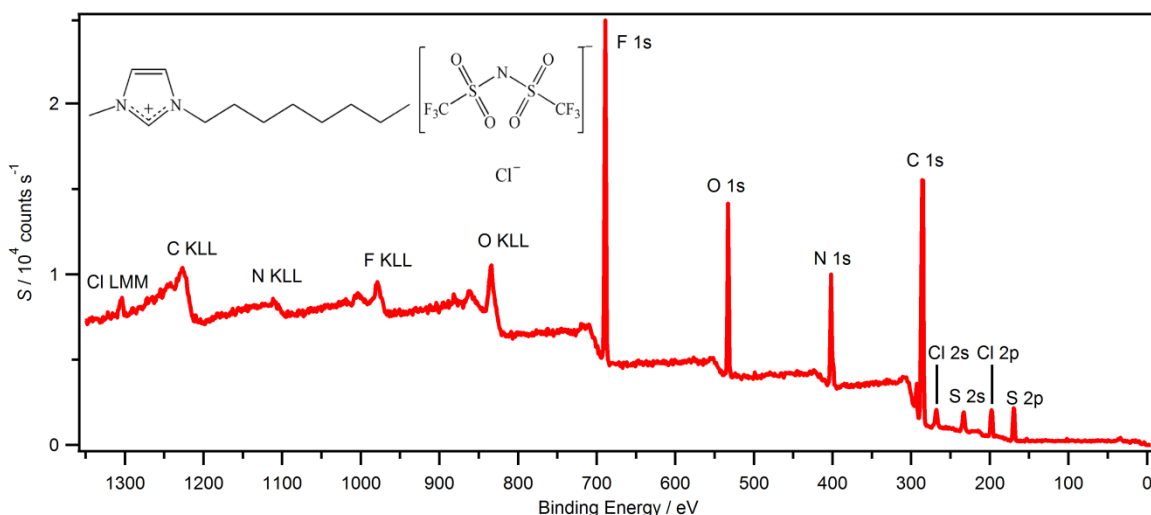


Figure S1: Survey XP spectrum for the equimolar mixture (1:1) of [C₈C₁Im]Cl:[C₈C₁Im][Tf₂N] ([C₈C₁Im]Cl_{0.5}[Tf₂N]_{0.5}).

Fitting of XP spectra: A full description of the peak deconstruction/fitting used to acquire the binding energy data provided in this publication can be found elsewhere.^{8a,10} Fitting procedures for all elements within $[\text{C}_8\text{C}_1\text{Im}]\text{Cl}$, $[\text{C}_8\text{C}_1\text{Im}][\text{TfO}]$, $[\text{C}_8\text{C}_1\text{Im}][\text{Tf}_2\text{N}]$ and $[\text{C}_8\text{C}_1\text{Im}][\text{OAc}]$ ionic liquids can also be seen in Figures S3-6 below. The same procedures were used to fit their characteristic peaks in the analysis of the XP spectra of their mixtures. An example of the fitting model used to deconstruct the C 1s XP spectrum of the $[\text{C}_8\text{C}_1\text{Im}]\text{Cl}_{0.5}[\text{Tf}_2\text{N}]_{0.5}$ mixture is shown in Figure S2. A brief description of the peaks typically observed in the high resolution XP spectra of the samples investigated in this work is presented here to aid further discussion of the results.

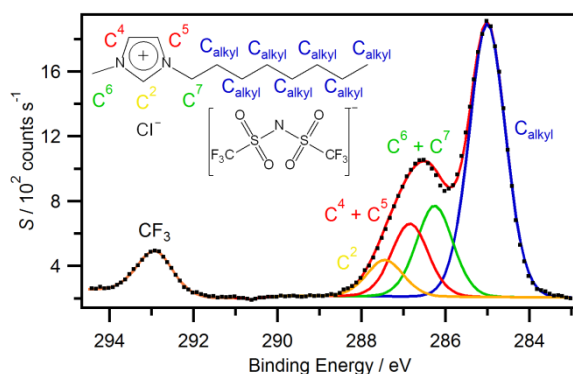


Figure S2. High resolution C 1s XP spectrum and fitting for the $[\text{C}_8\text{C}_1\text{Im}]\text{Cl}_{0.5}[\text{Tf}_2\text{N}]_{0.5}$ mixture. The C 1s high resolution XP spectrum of non-functionalised imidazolium-based ionic liquids is commonly composed of two partially resolved peaks (≈ 285 eV and ≈ 287 eV). In this spectrum a peak in the high binding energy region (≈ 292 eV) can also be observed, which is the signal from the CF_3 moiety in the anion. All XP spectra are charge corrected by setting $C_{\text{alkyl}} 1s = 285.0$ eV.

Upon inspection it is clear that the C 1s XP spectra for each of the ionic liquids studied here is dominated by two partially resolved photoemission peaks which are associated with the 1,3-dialkylimidazolium cation. The peak at higher binding energy (≈ 287 eV), is assigned to carbon atoms associated with the charged headgroup, *i.e.* the carbon atoms of the ring itself and those directly bonded to nitrogen (C^2 , C^4 , C^5 , C^6 and C^7 1s in the fitting model illustrated in Figure S2). The peak at lower binding energy (285.0 eV), labelled C_{alkyl} , is assigned to those carbon atoms located in the alkyl sidechain, the binding energy of this contribution is commonly used as a reference position when charge correcting experimental data. Additional anion based contributions are also

expected when the anion is also carbon containing. In the case of $[\text{Tf}_2\text{N}]^-$ and $[\text{TfO}]^-$ based samples, a well resolved photoemission peak in the high binding energy region (≈ 292 eV) is observed, this contribution is assigned to the CF_3 group of the respective anion. In the case of carboxylate based anions, *e.g.* $[\text{OAc}]^-$, anion based contributions are coincident with that of the cation. Consequently a modified fitting model must be employed, this gives rise to a suitable weighted model where the additional carbon is correctly allocated to an appropriate binding energy.¹⁰ For the neat $[\text{C}_8\text{C}_1\text{Im}]\text{Cl}$, shake-up satellites can also be observed as broad, relatively structureless features in the spectrum at 291.5-295.5 eV, a similar binding energy to the peak from the $-\text{CF}_3$ moiety.

The N 1s XP spectra of all the imidazolium based liquids studied exhibit a single photoemission peak for the nitrogen atoms within the cation (N_{cation} 1s). In samples containing $[\text{Tf}_2\text{N}]^-$ a second peak (half the intensity of N_{cation} 1s) is also noted at lower binding energy, this peak is assigned to the nitrogen atom in the anion. O 1s and F 1s XP spectra are composed of a single peak because all oxygen and fluorine atoms for the anions studied here have the same electronic environment. Cl 2p and S 2p XP spectra are both observed as spin orbit coupled doublets ($2p_{1/2}$ and $2p_{3/2}$) with peak separations of 1.6 and 1.2 eV respectively.

Charge correction: the acquisition of accurate binding energies is of utmost importance in this study. We have shown that absolute and comparable binding energies can be obtained after charge correction of the spectra using the C_{alkyl} 1s component of the C 1s spectrum; this method has been shown to be very reliable when the cation is substituted with alkyl chains containing a minimum of eight carbons.^{8a} All ionic liquids analysed in this study possess long alkyl substituents (*i.e.* all have a $[\text{C}_8\text{C}_1\text{Im}]^+$ cation), consequently the binding energies presented in this study are all acquired after setting the corresponding C_{alkyl} 1s signal = 285.0 eV.

Figures S3-6. Wide and fitted high resolution XP spectra of all $[\text{C}_8\text{C}_1\text{Im}][\text{X}]$ studied. C 1s high resolution XP spectra were fitted using the model described in the paper (Figure S2). All modelled components in F 1s, O 1s and N 1s high resolution XP spectra were fitted assuming equal full width at half maxima (FWHM). S 2p and Cl 2p high resolution XP spectra were fitted taking into account spin orbit coupling splittings of 1.2 eV for S 2p and 1.6 eV for Cl 2p.¹¹ The $p_{1/2}:p_{3/2}$ ratios were set to 1:2 and the FWHM are set to be equal for both $p_{1/2}$ and $p_{3/2}$ contributions.¹² For N 1s high resolution XP spectra, the N_{cation} 1s signal is affected by the shake up/off phenomena and was fitted with a 12 % intensity loss with respect to other peaks.¹³

Figure S3 [C₈MIM][Tf₂N] wide and high resolution scans.

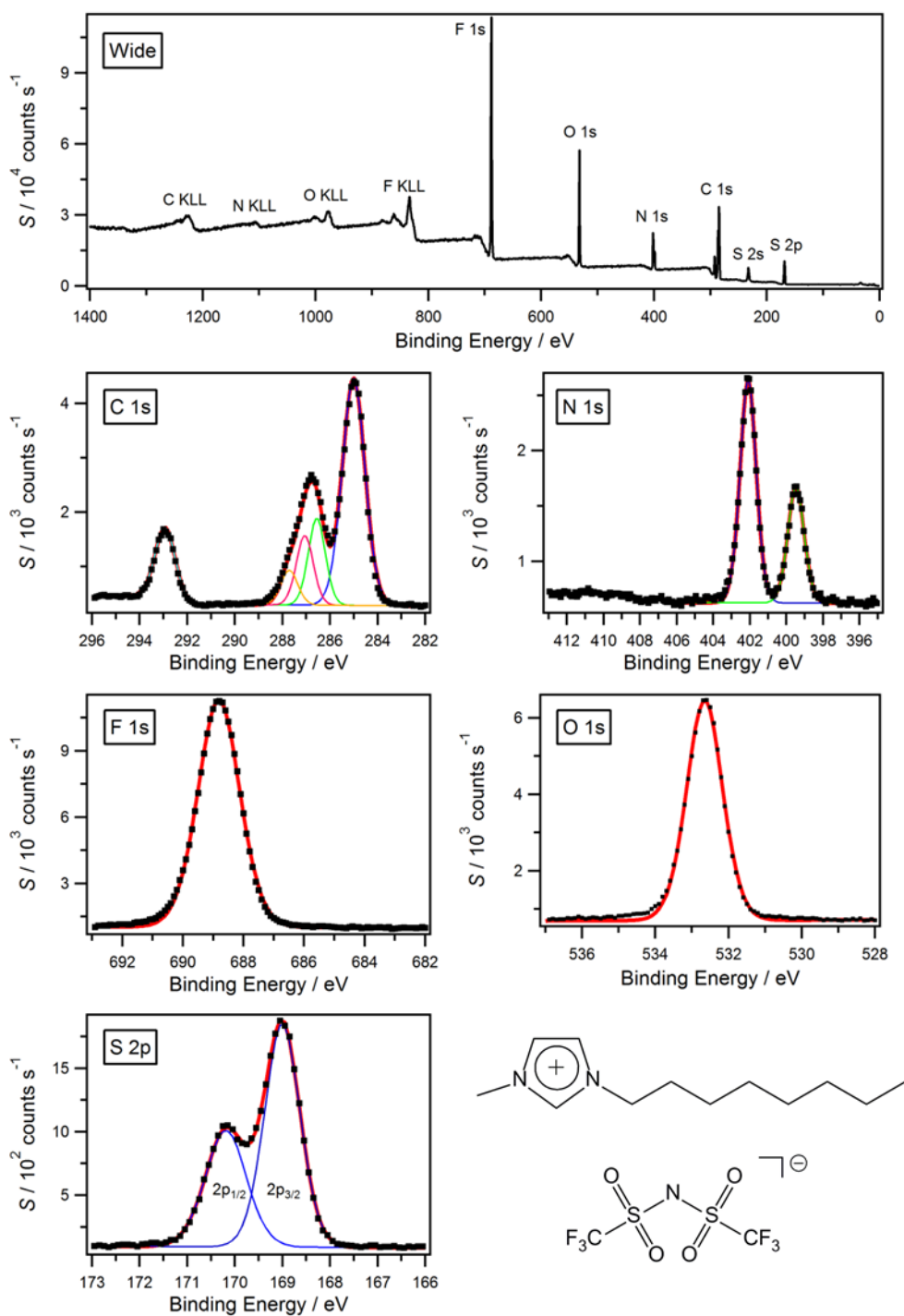


Figure S4 [C₈MIM][CF₃SO₃] wide and high resolution scans.

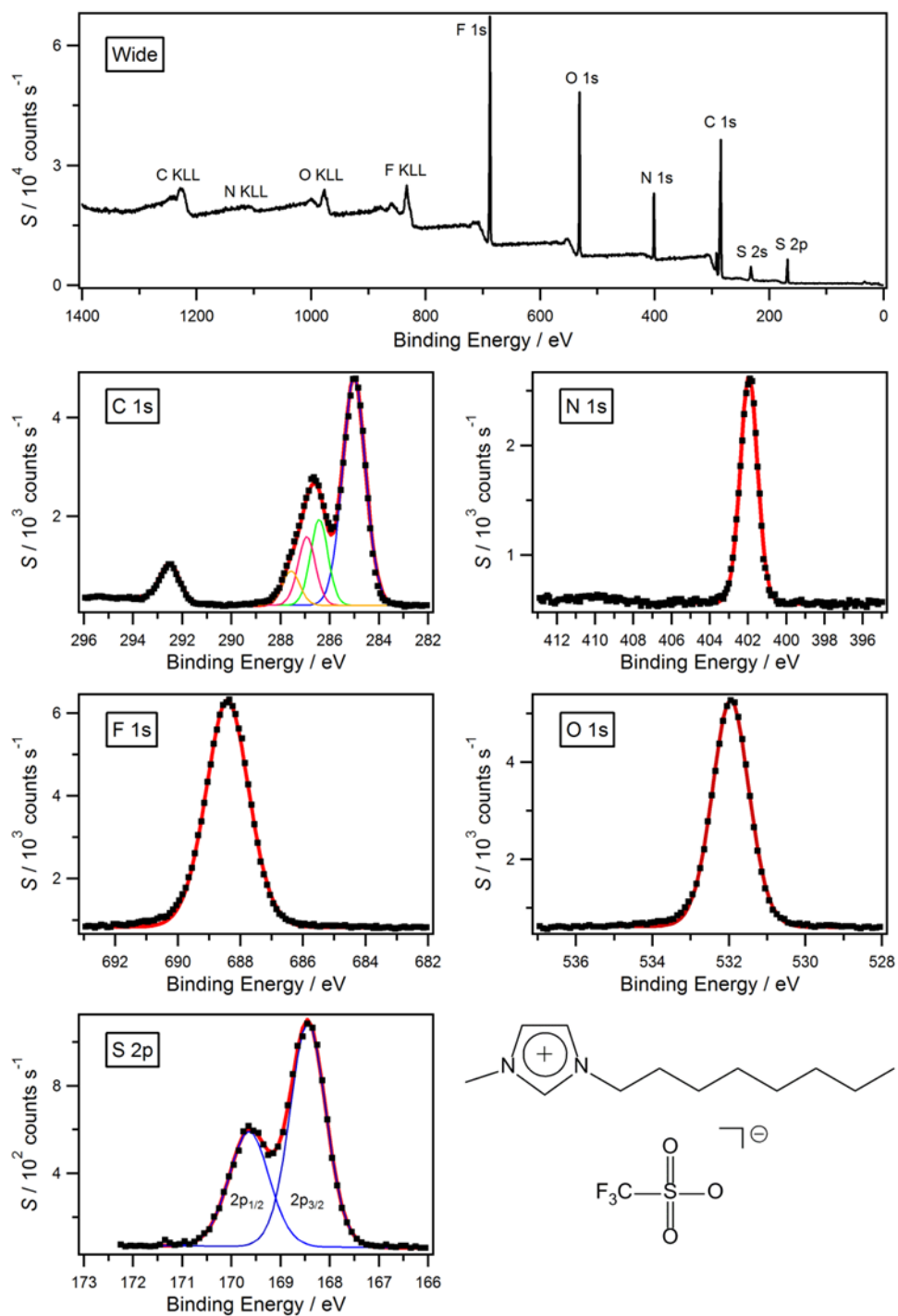


Figure S5 [C₈MIM]Cl wide and high resolution scans.

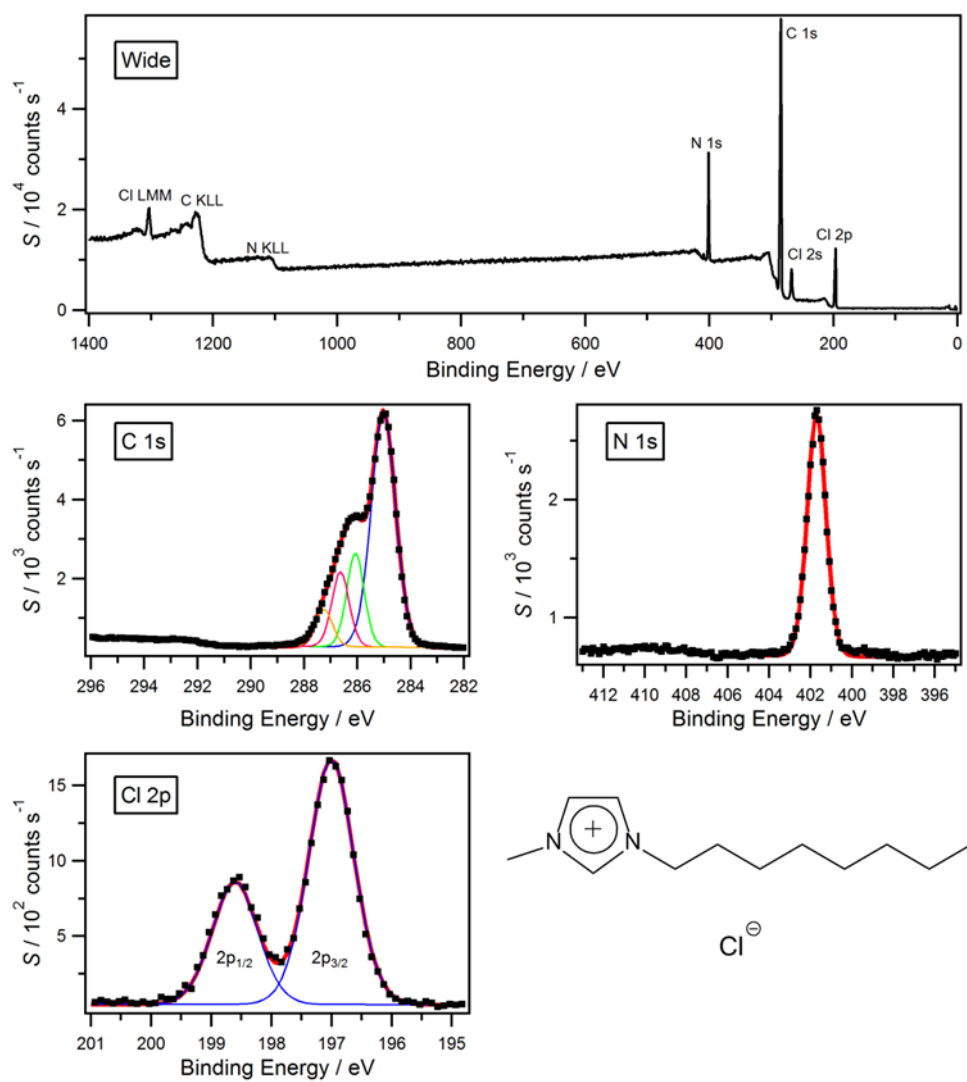


Figure S6 [C₈MIM][OAc] wide and high resolution scans.

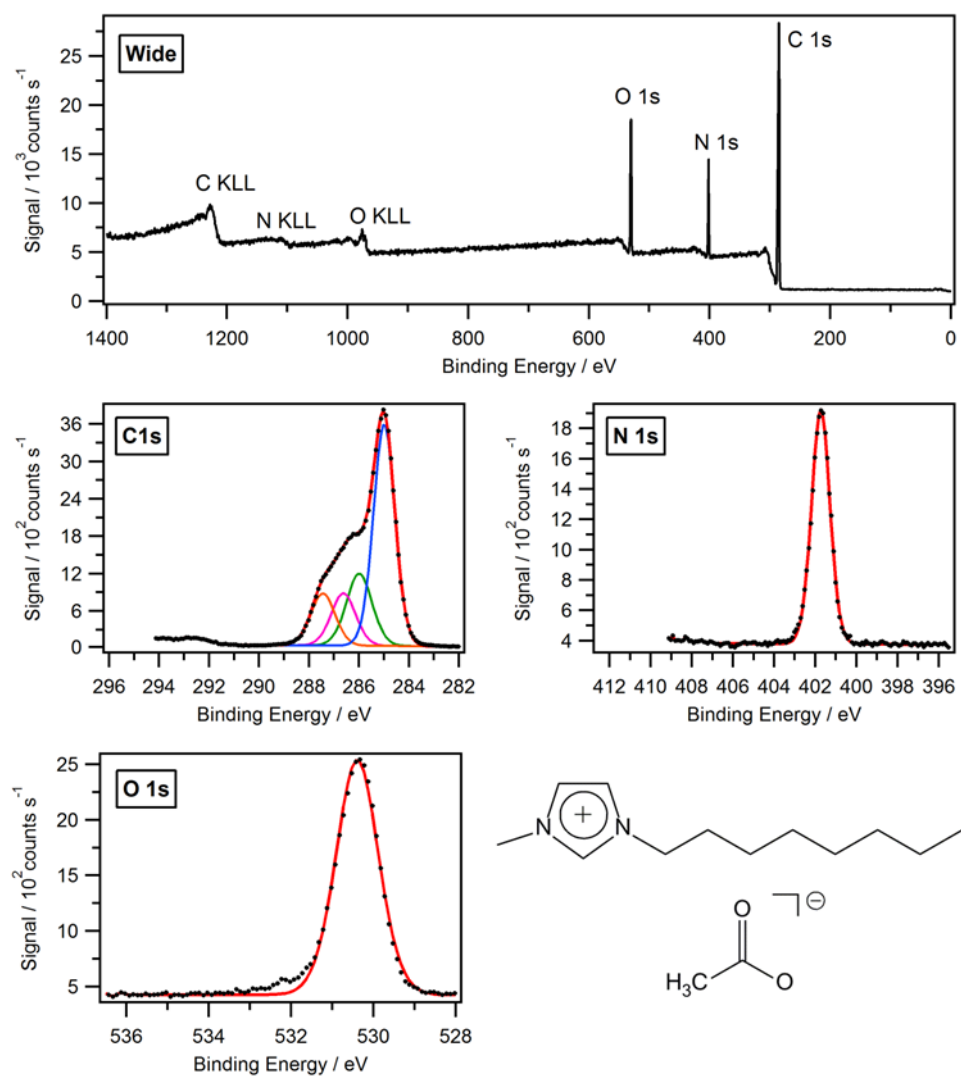


Figure S7a. FWHM of all $[\text{C}_8\text{C}_1\text{Im}]\text{Cl}:[\text{C}_8\text{C}_1\text{Im}][\text{Tf}_2\text{N}]$ mixtures. FWHM values are similar for the fitting of all different mixtures and the neat ionic liquid XPS analyses confirming that the signals measured are coming from just one environment.

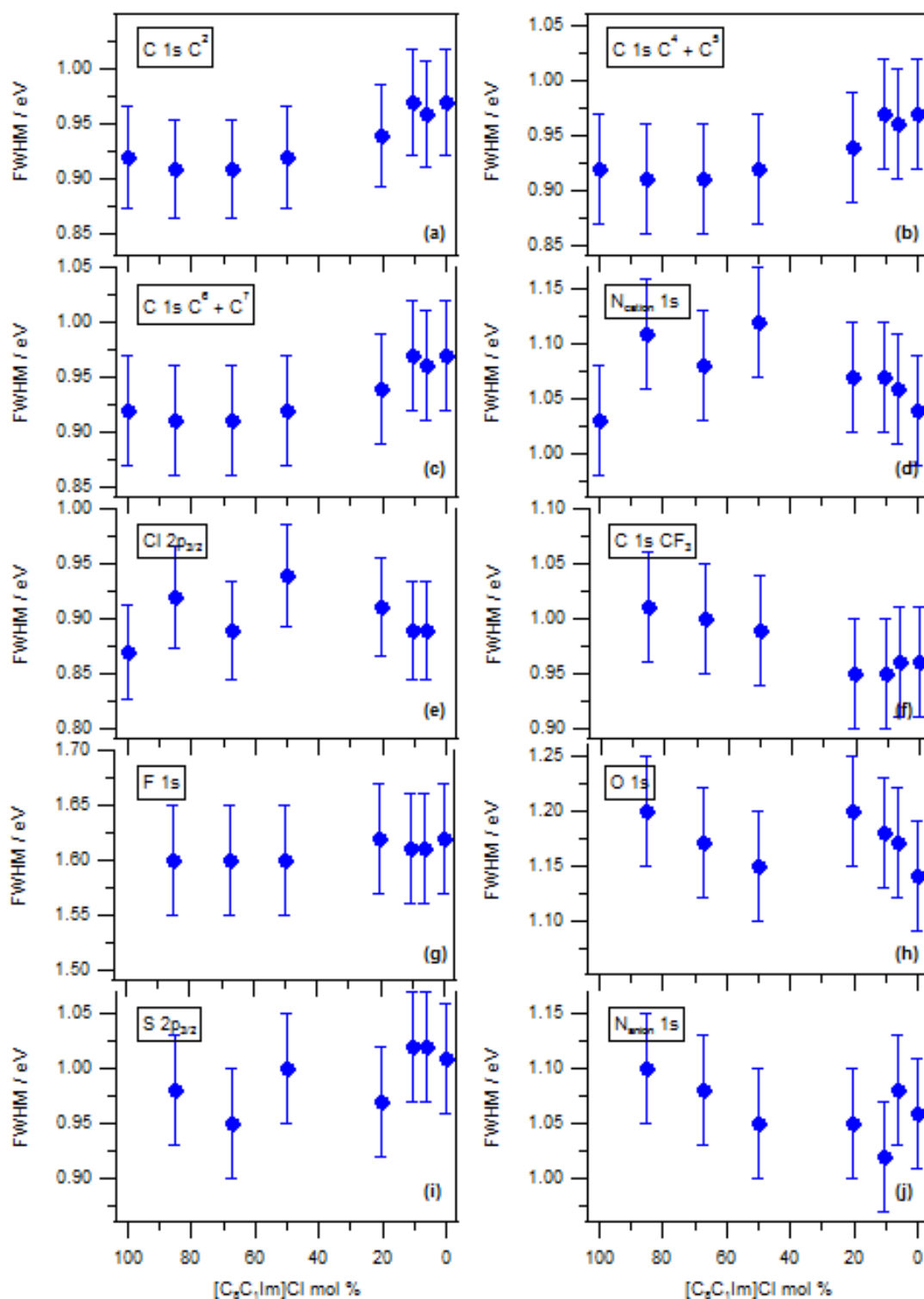


Figure S7b. FWHM of all $[\text{C}_8\text{C}_1\text{Im}]\text{Cl}:[\text{C}_8\text{C}_1\text{Im}][\text{OAc}]$ mixtures. FWHM values are similar for the fitting of all different mixtures and the neat ionic liquid XPS analyses confirming that the signals measured are coming from just one environment.

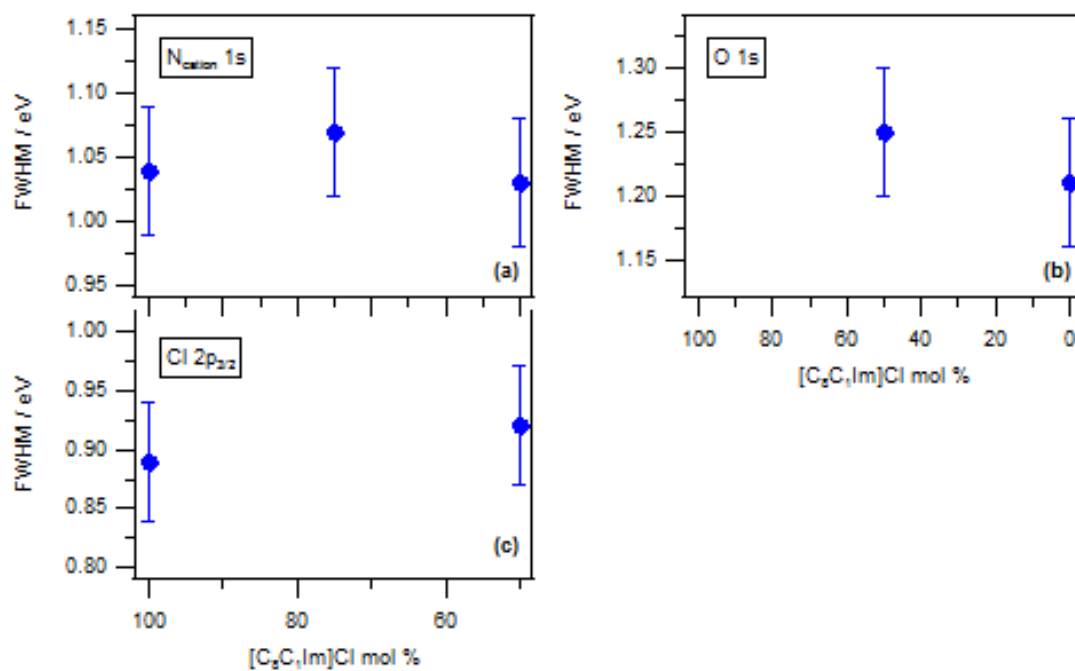


Figure S7c. FWHM of all $[\text{C}_8\text{C}_1\text{Im}]\text{Cl}:[\text{C}_8\text{C}_1\text{Im}][\text{TfO}]$ mixtures. FWHM values are similar for the fitting of all different mixtures and the neat ionic liquid XPS analyses confirming that the signals measured are coming from just one environment.

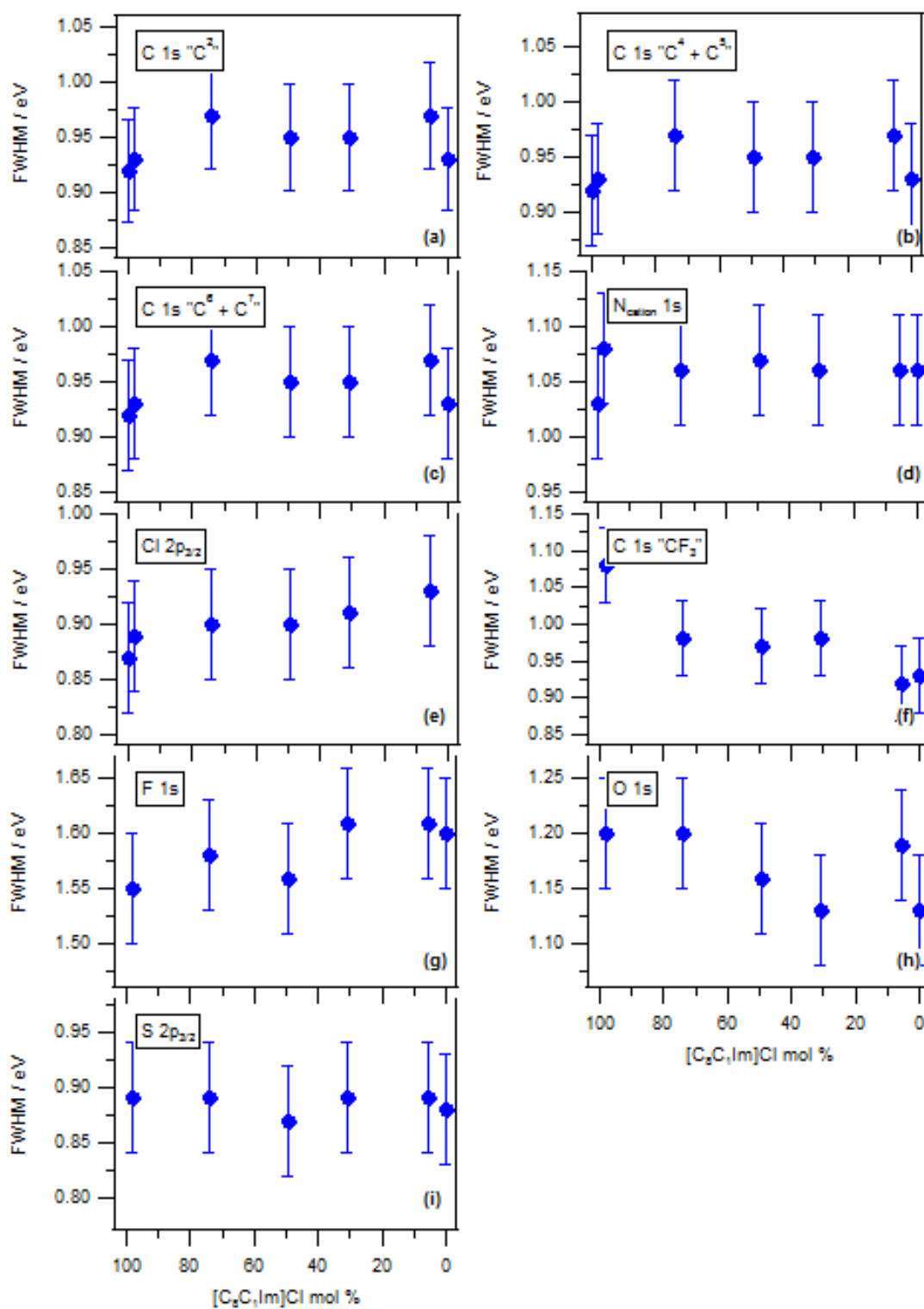


Figure S8 (a) C 1s C² (b) C 1s C⁴ + C⁵ (c) C 1s C⁶ + C⁷ (d) N_{cation} 1s (e) Cl 2p_{3/2} (f) CF₃ 1s (g) F 1s (h) O 1s (i) S 2p_{3/2} binding energies for [C₈C₁Im]Cl_x[TfO]_{1-x} mixtures. The y-axis scales for binding energy are all the same range, making comparisons easier; hence, the error bars (± 0.1 eV) are all the same height.

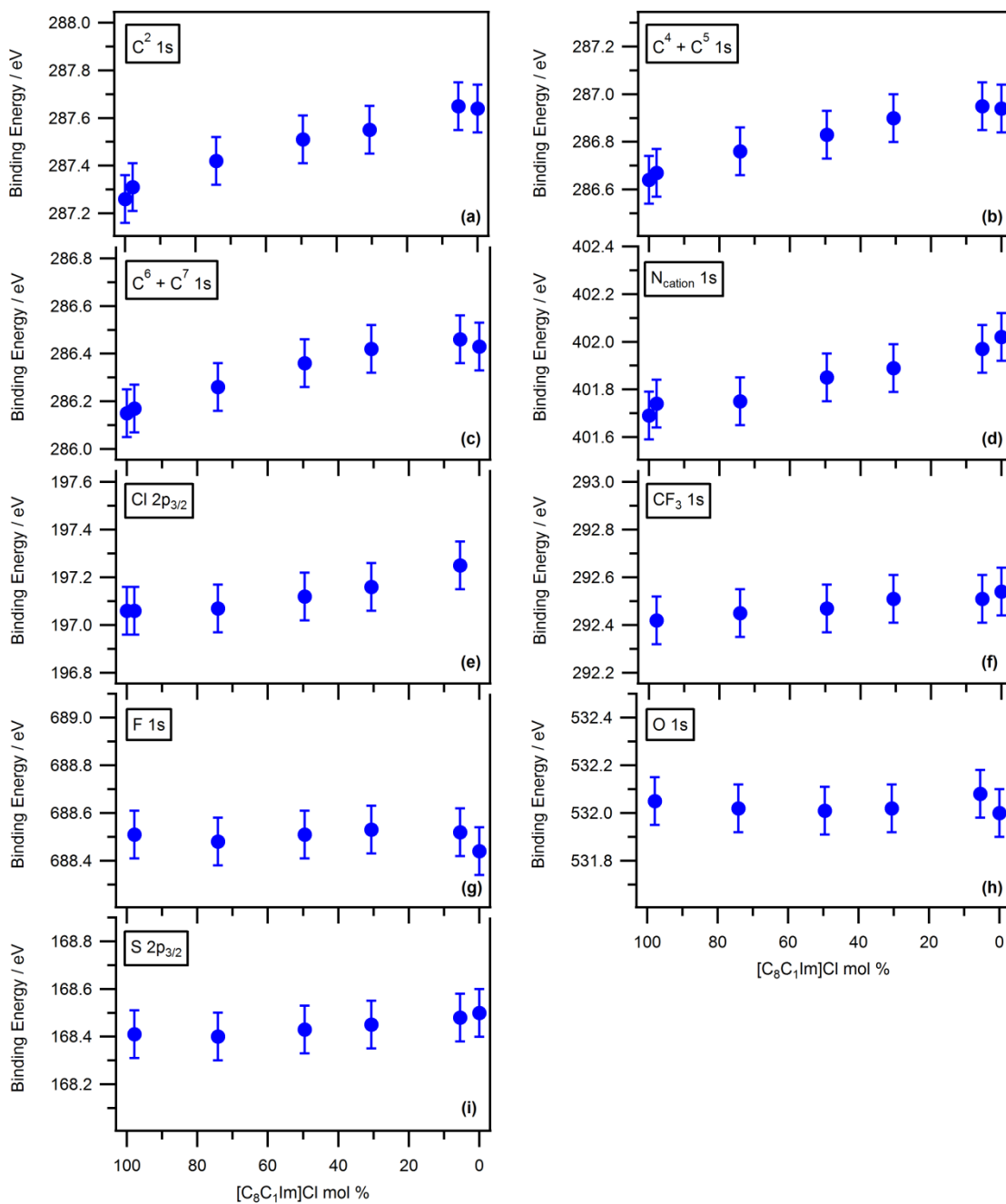
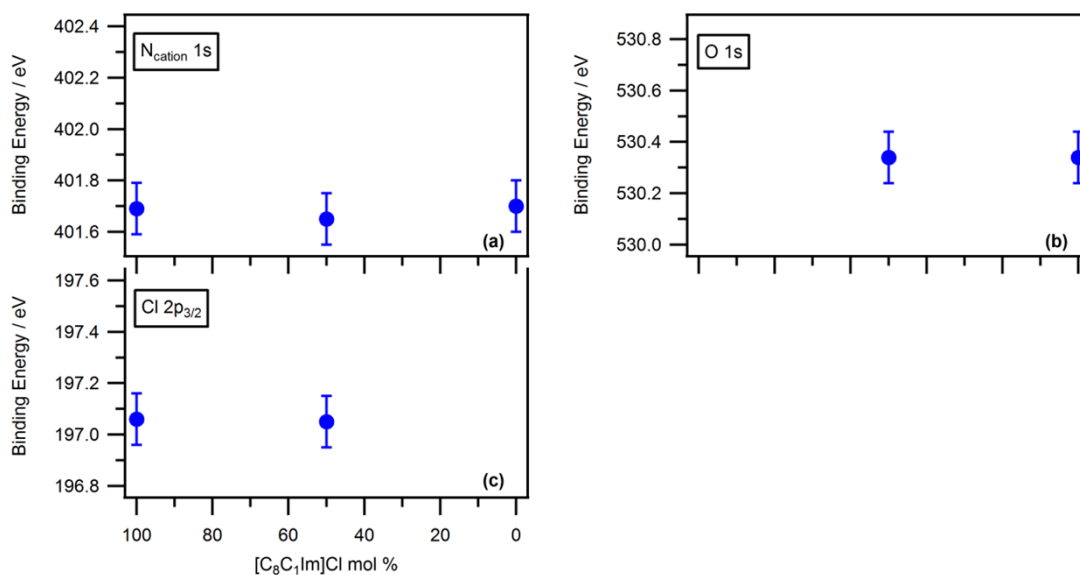


Figure S9 (a) C 1s C² (b) C 1s C⁴ + C⁵ (c) C 1s C⁶ + C⁷ (d) N_{cation} 1s (e) Cl 2p_{3/2} (f) CF₃ 1s (g) F 1s (h) O 1s (i) S 2p_{3/2} binding energies for [C₈C₁Im]Cl_x[OAc]_{1-x} mixtures. The y-axis scales for binding energy are all the same range, making comparisons easier; hence, the error bars (± 0.1 eV) are all the same height.



References:

- (1) Huddleston, J. G.; Visser, A. E.; Reichert, W. M.; Willauer, H. D.; Broker, G. A.; Rogers, R. D. *Green Chem.* **2001**, *3*, 156.
- (2) Bonhote, P.; Dias, A. P.; Papageorgiou, N.; Kalyanasundaram, K.; Gratzel, M. *Inorg. Chem.* **1996**, *35*, 1168.
- (3) Tokuda, H.; Hayamizu, K.; Ishii, K.; Abu Bin Hasan Susan, M.; Watanabe, M. *J. Phys. Chem. B* **2004**, *108*, 16593.
- (4) Brandt, A.; Hallett, J. P.; Leak, D. J.; Murphy, R. J.; Welton, T. *Green Chem.* **2010**, *12*, 672.
- (5) Taylor, A. W.; Lovelock, K. R. J.; Deyko, A.; Licence, P.; Jones, R. G. *Phys. Chem. Chem. Phys.* **2010**, *12*, 1772.
- (6) (a) Smith, E. F.; Rutten, F. J. M.; Villar-Garcia, I. J.; Briggs, D.; Licence, P. *Langmuir* **2006**, *22*, 9386(b) Wagner, C. D.; Davis, L. E.; Zeller, M. V.; Taylor, J. A.; Raymond, R. H.; Gale, L. H. *Surf. Interface Anal.* **1981**, *3*, 211.
- (7) *Surface Analysis by Auger and X-ray Photoelectron Spectroscopy*; Briggs, D.; Grant, J. T., Eds.; IM Publications: Manchester, 2003.
- (8) (a) Villar-Garcia, I. J.; Smith, E. F.; Taylor, A. W.; Qiu, F. L.; Lovelock, K. R. J.; Jones, R. G.; Licence, P. *Phys. Chem. Chem. Phys.* **2011**, *13*, 2797(b) Men, S.; Lovelock, K. R. J.; Licence, P. *Phys. Chem. Chem. Phys.* **2011**, *13*, 15244.
- (9) (a) Lovelock, K. R. J.; Smith, E. F.; Deyko, A.; Villar-Garcia, I. J.; Licence, P.; Jones, R. G. *Chem. Commun.* **2007**, 4866(b) Lovelock, K. R. J.; Kolbeck, C.; Cremer, T.; Paape, N.; Schulz, P. S.; Wasserscheid, P.; Maier, F.; Steinrück, H. P. *J. Phys. Chem. B* **2009**, *113*, 2854(c) Smith, E. F.; Villar Garcia, I. J.; Briggs, D.; Licence, P. *Chem. Commun.* **2005**, 5633(d) Gottfried, J. M.; Maier, F.; Rossa, J.; Gerhard, D.; Schulz, P. S.; Wasserscheid, P.; Steinrück, H. P. *Z Phys Chem* **2006**, *220*, 1439(e) Hashimoto, H.; Ohno, A.; Nakajima, K.; Suzuki, M.; Tsuji, H.; Kimura, K. *Surf. Sci.* **2010**, *604*, 464.
- (10) Hurisso, B. B.; Lovelock, K. R. J.; Licence, P. *Phys. Chem. Chem. Phys.* **2011**, *13*, 17737.
- (11) Moulder, J. F.; Stickle, W. F.; Sobol, P. E.; Bomben, K. D. *Handbook of X-ray photoelectron spectroscopy: a reference book of standard spectra for identification and interpretation of XPS data*; Physical Electronics: Eden Prairie, 1995.
- (12) Nesbitt, H. W.; Bancroft, G. M.; Davidson, R.; McIntyre, N. S.; Pratt, A. R. *Am. Mineral.* **2004**, *89*, 878.
- (13) Villar-Garcia, I. J. Ph.D. Thesis, University of Nottingham, 2009.